

Laughlin-Jastrow-correlated Wigner crystal in a strong magnetic field

Hangmo Yi and H.A. Fertig

Department of Physics and Astronomy and Center for Computational Sciences, University of Kentucky, Lexington, KY 40506
(May 11, 2018)

We propose a new ground state trial wavefunction for a two-dimensional Wigner crystal in a strong perpendicular magnetic field. The wavefunction includes Laughlin-Jastrow correlations between electron pairs, and may be interpreted as a crystal state of composite fermions or composite bosons. Treating the power m of the Laughlin-Jastrow factor as a variational parameter, we use quantum Monte Carlo simulations to compute the energy of these new states. We find that our wavefunctions have lower energy than existing crystalline wavefunctions in the lowest Landau level. Our results are consistent with experimental observations of the filling factor at which the transition between the fractional quantum Hall liquid and the Wigner crystal occurs for electron systems. Exchange contributions to the wavefunctions are estimated quantitatively and shown to be negligible for sufficiently small filling factors.

PACS numbers: 73.40.Hm, 73.20.Dx

I. INTRODUCTION

It was first argued by Wigner in 1934 that a system of interacting but otherwise structureless electrons can have crystalline order in the limit of low density and low temperature¹. The first experimental evidence of the Wigner crystal (WC) was found well over 40 years later in a two-dimensional (2D) system of electrons adsorbed on a helium surface². Nowadays, semiconductor heterojunction devices are considered a very promising environment for observing the WC. The advantage of heterojunction structures comes from the fact that the 2D electron plane is spatially separated from the donor layer, so that the influence of these impurities can be substantially reduced compared to bulk semiconductor environments. Furthermore, it is now well known that a strong magnetic field perpendicular to the 2D plane can effectively localize electron wavefunctions while keeping the kinetic energy controlled³⁻⁵. Since this lessens the otherwise severe low-density condition, it is believed that the WC can be stabilized in a sufficiently strong magnetic field.

On the other hand, the fractional quantum Hall (FQH) liquid is known to be the ground state in certain ranges of strong magnetic field^{6,7}. In this strongly correlated liquid state, the Hall resistivity ρ_{xy} is quantized at discrete values and the diagonal resistivity ρ_{xx} vanishes at zero temperature. In contrast, ρ_{xx} presumably diverges at $T = 0$ in the pinned WC. The FQH effect for $\nu = 1/m$ (m odd) is now fairly well understood in terms of the Laughlin wavefunction⁸.

In several recent experiments with high mobility samples, a sharp phase transition from the FQH state to an insulating state was observed as the magnetic field was increased both in electron^{9,10} and hole¹¹ systems. Some properties of the insulating state such as the activation gap in charge transport closely resembles those of pinned charge density waves, supporting the interpretation of this insulating state as a WC. Theoretical calculations of both the FQH liquid energy¹² and the WC energy^{13,14}

are also in good agreement with the experiments as to the critical value of the magnetic field at which the transition occurs for a given electron density.

However, *not* all experimental findings of the insulating state are consistent with the conventionally accepted theoretical understandings of the WC. (I) First, there is a discrepancy in the energy of charged excitations. Particularly, transport experiments⁹ reveal that the activation gap is an order of magnitude smaller than the theoretically estimated energy to create a point defect in the WC¹⁵⁻¹⁷. (II) Moreover, even deep into the insulating phase, anomalous behavior is observed when the filling factor ν is an inverse odd integer, which may be related to the FQH effect. Specifically, transport experiments¹⁸ exhibit a dip in the diagonal resistivity ρ_{xx} of the insulating state near $\nu = 1/7$. Also, photoluminescence experiments¹⁹⁻²² exhibit structure near odd denominator filling factors down to $1/11$, which looks very similar to structure seen at higher fillings where the FQH effect occurs. (III) Finally, experiments^{18,23,24} show that the Hall resistivity ρ_{xy} in the insulating phase saturates at its classical value B/nec , just as in the FQH liquid phase. This behavior *cannot* be understood in terms of a model of thermally activated point defects that are essentially non-interacting²⁵. Interestingly, (II) and (III) suggest that some characteristics of the FQH effect are shared by the insulating state.

The unusual behavior of ρ_{xy} has led to speculation that the insulating phase is not a WC at all, but rather a disorder-dominated state called the “Hall insulator”^{26,27}. However, it has been shown that interstitial defects in a WC can also lead to Hall insulating behavior if one introduces Laughlin-Jastrow correlations between the interstitials and the lattice electrons^{25,28}. The correlation was found to lower the energy to create such defects. However, more careful studies²⁹ of the above interstitial state using Monte Carlo simulations suggest that in order to obtain such a small excitation energy as found in experiment, one must introduce Laughlin-Jastrow correlations into the ground state as well. In this paper we explore

the energetics of ground state wavefunctions of this form.

In what follows we will introduce trial wavefunctions that take the form of a Laughlin-Jastrow factor multiplying a properly (anti-)symmetrized product of single particle states. The wavefunction introduced here thus corresponds to composite fermion or boson states^{30,31}. The energies of these states are computed using quantum Monte Carlo simulations, and it will be demonstrated that such states are generically lower in energy than other lowest Landau level WC states in the literature. Our computational method in its simplest form ignores exchange corrections; i.e., the state multiplying the Laughlin-Jastrow factor is approximated as a simple product of single particle states. An in-principle exact computational scheme in which permutations of the single particle states are sampled shows that this is an excellent approximation, provided the filling factor is not too large.

This paper is organized as follows: The trial many body wavefunction of the Laughlin-Jastrow-correlated WC is introduced and some of its properties are discussed in Sec. II. In Sec. III, the ground state energy is computed using a Monte Carlo simulation. Various aspects of the results are also discussed. Sec. IV is devoted to discussions on the effect of the exchange energy and validity of our approximation. Finally, we summarize the findings in Sec. V. Some technical details of the energy calculation can be found in the Appendix.

II. TRIAL WAVEFUNCTION

The Hamiltonian of 2D electrons moving in a magnetic field \mathbf{B} and interacting with the Coulomb energy is written

$$H = \sum_i \frac{1}{2m} \left| \mathbf{p}_i - \frac{e}{c} \mathbf{A}(\mathbf{r}_i) \right|^2 + \frac{1}{2} \sum_{i \neq j} \frac{e^2}{|\mathbf{r}_i - \mathbf{r}_j|}, \quad (2.1)$$

where \mathbf{r}_i and \mathbf{p}_i are the 2D position and momentum of the i -th electron, and \mathbf{A} is the vector potential from which the magnetic field is given by $\mathbf{B} = \nabla \times \mathbf{A}$. We will ignore the spin degree of freedom assuming that it is completely polarized by the strong magnetic field.

Since our trial wavefunction is closely related to the Hartree-Fock wavefunction of the WC suggested in Ref. 32, it is worthwhile to summarize the aspects of the Hartree-Fock wavefunction here. Explicitly, it can be written

$$\Psi_{HF}(\{\mathbf{r}_i\}) = \mathcal{A} \prod_i \phi_{\mathbf{R}_i}^{HF}(\mathbf{r}), \quad (2.2)$$

where $\phi_{\mathbf{R}_i}^{HF}$ are single electron wavefunctions and \mathcal{A} antisymmetrizes the total many body wavefunction. To a first approximation in the large magnetic field, all electrons will lie completely in the lowest Landau level. The un-normalized single particle wavefunction is thus given by

$$\phi_{\mathbf{R}_i}^{HF}(\mathbf{r}) = e^{-\frac{|\mathbf{r}-\mathbf{R}_i|^2}{4\ell^2} - i\frac{\mathbf{r} \times \mathbf{R}_i \cdot \hat{z}}{2\ell^2}}. \quad (2.3)$$

This wave function describes an electron localized at \mathbf{R}_i within a 2D Gaussian wavepacket. The magnetic length $\ell = \sqrt{\hbar c/eB}$ determines the size of the wavepacket. The phase factor in Eq. (2.3) ensures that $\phi_{\mathbf{R}_i}^{HF}$ is a product of $e^{-|\mathbf{r}|/4\ell^2}$ and an analytic function of $z \equiv x + iy$, making it entirely lie in the lowest Landau level. In the large B limit, $\ell \rightarrow 0$, and the electrons become highly localized, behaving almost like classical point charges. The kinetic energy is given by the lowest Landau level energy $\hbar\omega_c/2 \equiv \hbar eB/2mc$, and is the same regardless of the Gaussian center \mathbf{R}_i . This allows one to treat \mathbf{R}_i as variational parameters in minimizing the total energy with respect to the Coulomb interaction. For a classical system, a triangular lattice is well known to have the lowest Coulomb energy for a given density³³. Therefore, in the limit $B \rightarrow \infty$, the ground state is expected to be represented by the above wavefunction, with \mathbf{R}_i forming a triangular lattice.

In a finite magnetic field, quantum fluctuations around the lattice sites become important and the above classical analogy is only approximate. Consequently, Ψ_{HF} is not guaranteed to give the lowest energy at finite \mathbf{B} . However, if \mathbf{B} is large enough, Ψ_{HF} is still very close to the true ground state. For this reason, it has been used even at finite \mathbf{B} by many authors, producing very good results. In this paper, however, we will improve upon it by introducing a correlation. Previous studies¹⁴ have introduced correlation factors that are exact for a harmonic Hamiltonian; however, such wavefunctions allow fluctuations in which particles may occasionally closely approach one another. A correlation factor which by now is well-known to suppress such fluctuations is the Laughlin-Jastrow factor: $\prod_{i < j} (z_i - z_j)^m$, where $z_i = x_i + iy_i$ is the complex notation of the electron coordinates. Because of the extra phase accumulated when one particle encircles a second, wavefunctions of this form may be understood as being comprised of particles that have m magnetic flux quanta attached to them. The idea of constructing wavefunctions of this general form was first suggested in the context of the FQH effect in groundbreaking work by Jain³⁰; the combination of electrons and an even number of flux quanta to form these wavefunctions have since become known as composite fermions. For odd values of m , the wavefunction multiplying the Jastrow factor must be symmetric under interchange of two particles, so that such states correspond to composite boson states³¹. The wavefunctions we study in this work may thus be interpreted as crystals of composite fermions or bosons.

We therefore propose the following trial wavefunction:

$$\Psi(\{\mathbf{r}_i\}) = \mathcal{A} \prod_{i \neq j} (z_i - z_j)^m \prod_i \phi_{\mathbf{R}_i}(\mathbf{r}_i) \quad (2.4)$$

Again, $\phi_{\mathbf{R}_i}$ is a single particle wavefunction which is localized at \mathbf{R}_i and lies in the lowest Landau level. Since we will consider finite size systems, only those lattice sites

within a disk of radius R_D will be included in the set of $\{\mathbf{R}_i\}$. In order to make the full wavefunction anti-symmetric, we choose to use either a Slater determinant (even m) or a symmetric sum of all possible permutations (odd m) for the single particle wavefunction part.

We cannot, however, simply use $\phi_{\mathbf{R}_i}^{HF}$ in Eq. (2.3) as our single particle wavefunctions, due to the following reason. Disregarding the antisymmetrization for the moment, the probability density is given by

$$|\Psi|^2 \sim \prod_{i \neq j} |\mathbf{r}_i - \mathbf{r}_j|^{2m} \prod_i |\phi_{\mathbf{R}_i}(\mathbf{r}_i)|^2 \quad (2.5)$$

$$= e^{2m \sum_{i \neq j} \log |\mathbf{r}_i - \mathbf{r}_j|} e^{2 \sum_i \log |\phi_{\mathbf{R}_i}(\mathbf{r}_i)|}. \quad (2.6)$$

As in Laughlin's "plasma analogy"⁸, $|\Psi|^2$ may be thought of as the Boltzmann distribution function for a "dual" classical system whose effective energy is given by the exponents in the above equation, up to an arbitrary effective temperature. The first exponent in Eq. (2.6) is identical to the 2D (logarithmic) Coulomb energy with coupling constant m . Each term in the second exponent describes an attractive effective potential centered at a lattice site \mathbf{R}_i . Obviously, if the effective Coulomb interaction were absent, the minimum of the effective energy would be achieved when $\mathbf{r}_i = \mathbf{R}_i$ for all i . However, due to the effective interaction, the static solution of \mathbf{r}_i will be moved away from \mathbf{R}_i , unless \mathbf{R}_i is the center of the disk. In general, the electrons will be pushed radially away from the center of the disk. Consequently, the whole system will spread out and the resulting electron density will be smaller than that of the intended lattice.

In order to prevent this unwanted expansion of the system, for each $\phi_{\mathbf{R}_i}$, we will introduce extra zeros ("ghost effective charges") outside the physical disk. The ghosts are introduced in such a way that if the real electrons were fixed at their lattice sites, the total of both real and ghost effective charges are symmetrically distributed about any given lattice site \mathbf{R}_i . In other words, the ghosts cause each lattice site to look like it is at the center of the system by "balancing" out the effective repulsive force of the surrounding electrons. As a consequence, each electron will remain centered near its own lattice site. Obviously, the specific positions of the ghosts depend on the lattice site \mathbf{R}_i . An example of the way ghosts are placed is shown in Fig. 1. Although outside the physical disk, the ghosts themselves occupy lattice sites. Including the ghosts, the single particle wavefunction is finally given by

$$\phi_{\mathbf{R}_i}(\mathbf{r}) = e^{-\frac{|\mathbf{r}-\mathbf{R}_i|^2}{4\ell^2} - i\frac{\mathbf{r} \times \mathbf{R}_i \cdot \hat{z}}{2\ell^2}} \prod_j (z - \eta_j^{(i)})^m \quad (2.7)$$

where $\eta_j^{(i)}$ are the complex coordinates of the ghosts that balance out the effective force at \mathbf{R}_i .

An interesting property of these wavefunctions is that the ghosts may be thought of as "renormalizing" the positions of lattice sites. To see this, one can rewrite Eq. (2.7) as

$$\begin{aligned} \phi_{\mathbf{R}_i}(\mathbf{r}) = & e^{-\frac{|\mathbf{r}-\mathbf{R}_i|^2}{4\ell^2} - i\frac{\mathbf{r} \times \mathbf{R}_i \cdot \hat{z}}{2\ell^2}} \\ & \times \exp \left[m \sum_j \log |z - \eta_j^{(i)}| \right. \\ & \left. + im \sum_j \arg(z - \eta_j^{(i)}) \right]. \end{aligned} \quad (2.8)$$

Once again in the plasma analogy, the logarithms in the exponent describe a 2D Coulomb potential caused by effective point charges with charge m . Now let us approximate the point charges $\{\eta_j\}$ by a uniform charge distribution whose density is the same as the average density of the original point charges. To do this, we write the sums in the argument of the exponential in the form

$$\begin{aligned} & m \sum_j \{ \log |z - \eta_j| + i \arg(z - \eta_j) \} \\ & \equiv m \int d^2\eta \{ \log |z - \eta| + i \arg(z - \eta) \} \rho_G(\eta) \end{aligned} \quad (2.9)$$

where $\rho_G(\eta)$ is the density of ghost particles. We then approximate

$$\rho_G(\eta) \approx \begin{cases} \bar{\rho} & \text{if } |\eta| > R_D \text{ and } |\vec{\eta} - \vec{R}_i| < R_G, \\ 0 & \text{otherwise,} \end{cases} \quad (2.10)$$

where $\bar{\rho}$ is the average electron density, R_D is the radius of the physical disk of the finite size system, and R_G is the radius of a "ghost disk", which must satisfy $R_G > 2R_D$. Provided r is well away from the physical disk edge, this approximation should be quite good, and we expect corrections to scale as $(r/R_D)^2$. Since the real part of the integral corresponds to the potential of a uniform charge density $m\bar{\rho}$ in a disk of radius R_G , with a circular hole of radius R_D , the real part of the integral may be computed using Gauss' law for two-dimensional electrostatics. The imaginary part of the integral may be computed analytically as well for $r \ll R_D$, yielding the approximated wavefunction

$$\begin{aligned} \phi'_{\mathbf{R}_i}(\mathbf{r}) = & e^{-\frac{|\mathbf{r}-\mathbf{R}_i|^2}{4\ell^2} - i\frac{\mathbf{r} \times \mathbf{R}_i \cdot \hat{z}}{2\ell^2}} \\ & \times \exp \left[\frac{\pi m \bar{\rho}}{2} (|\mathbf{r} - \mathbf{R}_i|^2 - |\mathbf{r}|^2) \right. \\ & \left. - i\pi m \bar{\rho} \mathbf{r} \times \mathbf{R}_i \cdot \hat{z} \right] \end{aligned} \quad (2.11)$$

$$= e^{-\frac{|\mathbf{r} - (1-m\nu)\mathbf{R}_i|^2}{4\ell^2} - i\frac{\mathbf{r} \times (1-m\nu)\mathbf{R}_i \cdot \hat{z}}{2\ell^2}} e^{-\frac{m\nu(1-m\nu)|\mathbf{R}_i|^2}{4\ell^2}}. \quad (2.12)$$

Note that because the amplitude and phase of $\phi'_{\mathbf{R}_i}$ have been treated on an equal footing, this wavefunction lies in the lowest Landau level. Ignoring the unimportant constant, $\phi'_{\mathbf{R}_i}$ describes an electron in the lowest Landau level, centered at a renormalized lattice site $(1-m\nu)\mathbf{R}_i$. Thus the "bare" lattice described by filling $\phi'_{\mathbf{R}_i}$ states will be smaller than the real lattice by a factor of $1-m\nu$.

The physical lattice however is spread back to its original size due to the Laughlin-Jastrow correlation. Therefore, the above “renormalization” of the lattice compensates for the previously mentioned lattice expansion due to the Laughlin-Jastrow factor.

Before we describe the energy calculation for our wavefunctions, let us briefly discuss about the effect of the Laughlin-Jastrow correlation to the characteristics of the WC, particularly in connection with the excitation energy. In a recent experiment⁹, Jiang et al., have measured the temperature dependence of the diagonal resistance in the reentrant insulating phase slightly above $\nu = 1/5$. According to their data, the activation gap for charge transport is given by $E_g \sim 0.63\text{K}$. Surprisingly, this energy is much smaller than would be theoretically expected. For example, using states of point particles whose positions are chosen to optimize the energy, the energy to create a point defect such as an interstitial or a vacancy has been estimated by many authors^{15–17}, but all the results are an order of magnitude greater than the above value of E_g . A more recent study of point defects, however, shows that the energy can be lowered if the Laughlin-Jastrow correlation is introduced between the interstitials and the lattice electrons²⁸. Our initial studies of interstitial wavefunctions using quantum Monte Carlo techniques such as those presented here suggest that to reach the very low activation energies seen in experiment, one needs to include Laughlin-Jastrow correlations among the ground state electrons as well^{29,34}. A discussion of such wavefunctions is deferred to a future publication.

III. COULOMB ENERGY: MONTE CARLO SIMULATION

Since our wavefunction lies completely in the lowest Landau level, we only need to minimize the Coulomb interaction term in the Hamiltonian. The expectation value of the Coulomb energy per electron is written

$$\frac{E_c}{N} = \frac{1}{2N} \sum_{i \neq j} \left\langle \frac{e^2}{|\mathbf{r}_i - \mathbf{r}_j|} \right\rangle \quad (3.1)$$

$$= \frac{e^2}{2N} \int d\mathbf{r} d\mathbf{r}' \frac{\left\langle \sum_{i \neq j} \delta(\mathbf{r} - \mathbf{r}_i) \delta(\mathbf{r}' - \mathbf{r}_j) \right\rangle}{|\mathbf{r} - \mathbf{r}'|}, \quad (3.2)$$

$$= \frac{e^2}{2} \int_C d\mathbf{r} \int d\mathbf{r}' \frac{\left\langle \sum_{i \neq j} \delta(\mathbf{r} - \mathbf{r}_i) \delta(\mathbf{r}' - \mathbf{r}_j) \right\rangle}{|\mathbf{r} - \mathbf{r}'|}, \quad (3.3)$$

where $\langle \dots \rangle$ means the expectation value with respect to the wavefunction Ψ in Eq. (2.4). In the last line, we have dropped $1/N$ and restricted the first integral within a single primitive cell at the center of the disk (denoted by C), using the lattice symmetry. Since the size of the simulated system is inevitably finite, in order to obtain the thermodynamic limit, we need to either extrapolate finite

size results, or use the Ewald sum method^{33,35}. We have used the second method in this paper. Details of the calculation are given in Appendix A, but it must be noted here that we have introduced a couple of approximations in calculating the Coulomb energy: (I) We have ignored the exchange energy, which in practice means that the antisymmetrization in Eq. (2.4) is dropped. We have tested this approximation and find that it is quite good unless ν is too close to $1/m$. The effect of exchange energy will be discussed in the next section in more detail. (II) Since $|\Psi|^2$ when unsymmetrized corresponds to a finite temperature classical Boltzmann weight, we assume there exists a length scale ξ_c above which fluctuations in the electron positions are uncorrelated. We thus use the Monte Carlo method to compute the Coulomb interaction between the charge density in the central unit cell and the charge out to some distance R_S which we presume to be larger than ξ_c . This run is also used to compute the charge density in the central primitive unit cell. In order to minimize boundary effects, we choose R_D , the radius of the disk containing all simulated dynamical electrons, to be greater than R_S , so that electrons close to R_S do not experience an environment significantly different than those in the bulk. Those electrons between radius R_S and R_D , which are dynamically simulated but not used to compute the energy, provide an “effective medium”. This approach has also been employed in Monte Carlo studies of the FQH effect³⁶.

The interaction of the charge density in the central unit cell with charge at distances greater than R_S is computed by treating the distant charge as static and equal to periodic copies of the numerically computed charge density in the central primitive cell. This is essentially a Hartree approximation. Since this charge density is treated as static, one may compute the interaction for an infinitely large system using the Ewald sum technique. Our method is checked by increasing R_S until the energy is unchanged within the errorbars of our Monte Carlo calculations. Our simulations show that for the wavefunction parameters we have studied, ξ_c is always less than $4a$, where a is the lattice constant. This is also confirmed by numerical calculations of individual pair energies, for which the result from the simulation is essentially the same as the Hartree energy if the pair is separated farther than $4a$. More details of this procedure are discussed in Appendix A.

We have developed a Monte Carlo simulation program that computes the Coulomb energy per electron, E_c/N , using the standard Metropolis algorithm³⁷. As a critical test of our extrapolation technique, we have used our method to compute the energy of the $m = 0$ state, which is identical to the one used in Ref. 32. Its energy can be calculated analytically and our results agree with analytic solutions well within the statistical errorbar of about 0.05%. The results for more interesting values of m are plotted in Fig. 2. Treating m as a variational parameter, one can find the value of m which gives the lowest energy at a given ν . The graph clearly shows that at

$\nu = 1/3$ and $1/5$, the Laughlin state has a lower Coulomb energy than any of our wavefunctions. At $\nu = 1/7$, however, the Laughlin state has a higher Coulomb energy than our lowest result. This is consistent with experiment in that the “true” FQH effect — e.g., vanishing diagonal resistivity ρ_{xx} at zero temperature — has never been observed at any inverse odd filling factors below $\nu = 1/5$. Furthermore, at $\nu = 1/5$, the energy of our wavefunction is higher than, but very close to that of the Laughlin state, which agrees well with the observation of a reentrant insulating phase⁹ slightly above $\nu = 1/5$. This reentrant phase is believed to occur because the pure Laughlin wavefunction is the ground state only when ν is *precisely* an inverse odd integer. Away from the precise filling factors, quasiparticles and quasiholes are present in the ground state, increasing the energy. Therefore the FQH states have cusps in energy at every inverse odd filling factor, allowing the WC state to have lower energy in a small but finite range of ν right *above* $1/5$.

Now, let us compare our results with other WC trial wavefunctions, particularly the Lam-Girvin form¹⁴. The Lam-Girvin wavefunction also predicts that the phase transition from the WC to the FQH effect occurs between $\nu = 1/5$ and $1/7$. As shown in Fig. 2, however, our wavefunctions are lower in energy than the Lam-Girvin counterpart at all values of ν where data is available. In other words, our wavefunctions are closer to the true ground state. We believe this difference arises because the harmonic approximation neglects rare, but nonetheless important contributions from anharmonic fluctuations in which two or more electrons come close together. In contrast, the Laughlin-Jastrow correlation very effectively suppresses density fluctuations at all displacements of electrons from the lattice sites. This may be understood using the plasma analogy for the Laughlin states⁸, i.e., the Laughlin-Jastrow correlation is equivalent to the Boltzmann distribution of a 2D one component plasma (OCP) in which charge density fluctuations are suppressed.

An important difference between the weighting associated with our wavefunction and the Boltzmann weight of the OCP is that the electrons are centered at different lattice sites in our wave function, while they are centered at one single point for the OCP. One of the most significant consequences of this is the following. Let us define $m_0(\nu)$ as the value of m for the lowest energy variational state at ν . Surprisingly, near an inverse odd integer filling factor, we find $\nu \sim 1/(2m_0 - 1)$ rather than $\nu \sim 1/m_0$ as in the Laughlin states. For example, at $\nu = 1/7$, our wavefunction has the lowest energy if $m = 4$, rather than $m = 7$. Now let us continue to focus on the $m = 4$ state increasing ν above $1/7$. It continues to be the lowest energy state until ν reaches about ~ 0.165 , where the $m = 3$ state becomes lower in energy. This implies a first order transition between the two different m states. This phase transition may in principle be detectable in photoluminescence experiments, although this is presumably difficult because the energies of neighboring m states are

so close together.

Fig. 3 shows Δr_{rms} , the root-mean-square value of the fluctuation of electrons from their lattice sites. Note that Δr_{rms} increases rapidly as ν approaches and passes beyond the transition to the $m - 1$ state. This indicates that the single electron probability density becomes less and less localized as ν increases. However, according to the above mentioned plasma analogy, the Laughlin-Jastrow factor still tries to force the local density to remain uniform. Therefore, rather than wandering around randomly, electrons tend to *switch* positions and form “exchange rings” (Fig. 4). This means that ring exchange energy becomes more and more important. This is most easily seen from “snap shots” of the electron configuration during a Monte Carlo simulation run. We note that such ring exchanges are commonly observed in simulations of melting of the classical OCP³⁹. In path integral descriptions of the FQH effect⁴⁰, coherence among ring exchanges play a crucial role in explaining the instability of the WC with respect to a liquid state at $\nu = 1/m$ for small enough m . We believe that quantum coherence in ring exchanges may lead to structure in the energy of the WC as a function of filling factor even in the insulating state, which ultimately could explain the transport and photoluminescence anomalies discussed in the introduction. However, a correct description of this requires that exchange be properly included; we therefore defer a detailed discussion of this to a future publication²⁹. As ν approaches and increases past the critical filling factor, the exchange rings are observed increasingly often in Monte Carlo snap shots. As ν increases further and Δr_{rms} grows to the same order of magnitude as the lattice constant, the WC will eventually become unstable, giving way to a liquid-like state. This is analogous to the melting transition of a conventional solid. In this limit, however, the exchange energy is clearly no longer negligible and our Monte Carlo analysis ceases to be valid. Then, an important question arises: when may exchange be ignored? We will address this question in the next section.

Now let us focus on the transitions between different m states. First, Fig. 3 shows characteristics of Δr_{rms} that is common to all m . In general, Δr_{rms} is an increasing function of ν , and as ν reaches some point, the system undergoes a phase transition to a lower m state. Interestingly, the values of Δr_{rms} at the critical ν is approximately given by the same value $\sim 1.7\ell$ regardless of m . We believe this implies that delocalization plays a crucial role determining where the transitions occur. Moreover, Fig. 2 shows that E_c/N starts to curve up as ν passes beyond the transition value, which is common for all m . We believe the delocalization and the formation of exchange rings are the main reasons for this change of curvature in the Coulomb energy. However, it is not yet clear why it occurs well below $\nu = 1/m$.

IV. EXCHANGE EFFECT: PERMUTATION MONTE CARLO SIMULATION

In the previous section, we have seen that the delocalization, which is represented by Δr_{rms} , increases as ν approaches $1/m$ from below. Then the exchange energy is expected to become more and more important, as the overlap of wavefunctions at different lattice sites increase. Indeed, we have more or less directly observed the formation of exchange rings in the snapshots from the Monte Carlo simulations for relatively large values of ν . Thus, it is clear that as ν grows, one must start to include the exchange energy in the calculation in order to obtain quantitatively reliable results.

It is very difficult to estimate the exchange energy analytically for our wavefunction mainly due to the strong correlations. However, when m is even, the single particle wavefunction part in Eq. (2.4) is a Slater determinant, and we can take the exchange energy into full account by using other Monte Carlo methods such as in Ref. 41. Our tests with the $m = 4$ state shows that the exchange energy is negligible when $\nu \lesssim 1/7$. Although this method treats the exchange energy exactly, its application is strictly restricted to even values of m , and we need to resort to a different method for odd m .

One way to estimate the relative importance of the exchange effect is as follows. The many body wavefunction in Eq. (2.4) may be rewritten

$$\Psi = \prod_{i \neq j} (z_i - z_j)^m \sum_P \zeta^P \phi_{\mathbf{R}_i}(\mathbf{r}_{P(i)}), \quad (4.1)$$

where the summation is over all possible permutations P . For an odd m , the statistical sign ζ^P is always $+1$, but for an even m , ζ^P is either $+1$ or -1 depending on whether P is an even or odd permutation. When we ignored the exchange effect in the previous section, what we did was to drop all permutations in the above summation, except the identity permutation I such that $I(i) = i$. In other words, we have approximated the above wavefunction with

$$\Psi_{\text{direct}} = \prod_{i \neq j} (z_i - z_j)^m \phi_{\mathbf{R}_i}(\mathbf{r}_i). \quad (4.2)$$

Now, we want to define a quantity γ , which measures error caused by this approximation, or in other words, measures how important the exchange effect is. First, the “partition function” maybe written

$$Z[\Psi] = \int |\Psi|^2, \quad (4.3)$$

where the integral is over all coordinates $\{r_i\}$. Then, we define

$$\gamma \equiv \left| \frac{Z[\Psi] - Z[\Psi_{\text{direct}}]}{Z[\Psi]} \right| \quad (4.4)$$

$$= \frac{\sum_{P \neq I} \int \prod_{i \neq j} |z_i - z_j|^{2m} \phi_{\mathbf{R}_i}(\mathbf{r}_i)^* \phi_{\mathbf{R}_i}(\mathbf{r}_{P(i)})}{\sum_P \int \prod_{i \neq j} |z_i - z_j|^{2m} \phi_{\mathbf{R}_i}(\mathbf{r}_i)^* \phi_{\mathbf{R}_i}(\mathbf{r}_{P(i)})}. \quad (4.5)$$

We have used the particle exchange symmetry to reduce the number of permutations in each integral from two to one. Note that when γ is small, the exchange effect is small and our approximation is good.

In order to compute γ numerically, we have developed a “permutation Monte Carlo method”⁴², which is essentially the same as the usual Monte Carlo simulation method, except for one important difference: In a permutation Monte Carlo simulation, not only the electron positions \mathbf{r}_i , but also the permutation P is treated as a configurational variable which is updated, tested, and accepted (or discarded) according to the Metropolis algorithm³⁷. Since the integrand in Eq. (4.5) is a complex quantity, we have separated the phase factor from the modulus to sample it. More specifically, we have averaged the phase factor

$$\frac{\phi_{\mathbf{R}_i}(\mathbf{r}_i)^* \phi_{\mathbf{R}_i}(\mathbf{r}_{P(i)})}{|\phi_{\mathbf{R}_i}(\mathbf{r}_i)^* \phi_{\mathbf{R}_i}(\mathbf{r}_{P(i)})|}, \quad (4.6)$$

using the rest of the factors in the integrand

$$\prod_{i \neq j} |z_i - z_j|^{2m} |\phi_{\mathbf{R}_i}(\mathbf{r}_i)^* \phi_{\mathbf{R}_i}(\mathbf{r}_{P(i)})| \quad (4.7)$$

as the statistical weight in the Monte Carlo simulation. We note that this permutation Monte Carlo scheme in principle captures the effects of symmetrization of the wavefunction exactly. In practice, however, the precision of the result depends on how accurately the phase may be sampled. As described below, this becomes problematic as $\nu \rightarrow 1/m$.

The results of the permutation Monte Carlo simulation is shown in Fig. 5. It is clear that γ is negligible if ν is less than 0.2, 0.16, and 0.14, for $m = 3, 4$, and 5, respectively. Beyond those values of ν , the exchange effect can be significant. The errorbars become quite large as the exchange effect gets more and more important. This is because except for the direct term, the phase factor in Eq. (4.6) fluctuates very much, while its average almost vanishes.

Note that we have found earlier from Fig. 2 that the transition between the $m = 4$ and the $m = 3$ states occurs near $\nu = 0.16$. Since the exchange effect is negligible up to $\nu = 0.16$ when $m = 4$, the $m = 4$ state is guaranteed to have a lower energy than the $m = 3$ state if $\nu \leq 0.16$, even if the exchange energy is included. Above $\nu = 0.16$, however, it is currently not known whether the exchange effect will raise or lower the total energy of the $m = 4$ state. If it lowers the energy, there is a possibility that the transition from $m = 4$ to $m = 3$ actually occur at a higher filling factor than is shown in Fig. 2. For $m = 5$, the exchange effect is negligible up to $\nu = 0.14$, which is well above $\nu = 0.125$ where the transition to the $m = 4$ state occurs. Therefore, for this transition, our estimate of the transition filling factor is accurate. In principle, however, it is possible that a *reentrant* $m = 5$ phase occurs within the $m = 4$ ground

state if the exchange effect brings the energy lower than that of the $m = 4$ state above $\nu = 0.14$. For $m = 3$, the exchange effect becomes important well before the energy level crosses with that of the $m = 2$ state. However, when $\nu \gtrsim 0.2$, not the WC, but the FQH state is the ground state, and the energy level crossing between different WC states is not physically relevant at $T = 0$. Finally, we note that for $m = 3$, the exchange terms are completely negligible when $\nu \leq 1/5$. Therefore, the comparison of the energy between our correlated WC state, the Laughlin state, and the Lam-Girvin state is valid at $\nu = 1/5$ as well as at $1/7$.

V. SUMMARY

In this paper, we have studied the correlated WC in a strong magnetic field, which is represented by the product wavefunction of the Laughlin-Jastrow factor and the Hartree-Fock wavefunction in a triangular lattice. We have shown that extra zeros (ghosts) in the single particle wavefunction are necessary to balance the expanding effect of the Laughlin-Jastrow correlation.

The energy of the wavefunction has been calculated using Monte Carlo simulations and the Ewald sum method. Compared to other WC trial wavefunctions in the lowest Landau level, particularly Lam-Girvin wavefunction, the new state is found to be the lowest in energy. The Laughlin FQH state has lower energy than our wavefunction at $\nu = 1/5$ and above, consistent with experiment in that the phase transition occurs between $\nu = 1/7$ and $1/5$. The energies of the two states are, however, very close to each other near $\nu = 1/5$. This is also consistent with the experimental observation of the reentrant insulating phase slightly above $\nu = 1/5$, considering the cusp in the FQH state energy due to quasiparticles and quasiholes.

Treating m as a variational parameter, we can find the value of m which gives our wavefunction the lowest energy. Since m takes only discrete integer values, it is found that there is a series of first order phase transitions between different m states as ν changes. For a given m , the spatial fluctuations of the electrons grows as ν increases above $\sim 1/(2m - 1)$, eventually causing the energy to curve up. Formation of exchange rings is also observed in this limit, which is reminiscent of what occurs near melting in classical one component plasmas.

We have also developed a permutation Monte Carlo method in order to estimate when the exchange effect becomes important. Our simulation shows that they are negligible up to $\nu = 0.2, 0.16$, and 0.14 for $m = 3, 4$, and 5 , respectively. This ensures validity of our comparison of the energy between different trial wavefunctions at $\nu = 1/5$ and $1/7$. It also shows that when the exchange energy is included, the filling factor at which the transition between the $m = 4$ and the $m = 3$ states occurs may be higher, but not lower than our estimate in this paper. However, for the transition from the $m = 5$ to the

$m = 4$ states, our estimate of the transition filling factor appears to be accurate.

ACKNOWLEDGMENTS

We wish to acknowledge J.J. Palacios, M.C. Cha, M.R. Geller, and I. Mihalek for helpful discussions. This work was supported by NSF grant DMR 95-03814.

APPENDIX A: THERMODYNAMIC LIMIT

In this appendix, we will explain how one can obtain the thermodynamic limit from the finite size simulation of the Coulomb energy. We first split the domain of the \mathbf{r}' integral in Eq. (3.3) into two regions

$$\int d\mathbf{r}' = \int_S d\mathbf{r}' + \int_U d\mathbf{r}'. \quad (\text{A1})$$

The first term is an integral over many, but a finite number of primitive cells near the center of the disk, which we call the ‘‘sampled primitive cells’’. In this region, the Coulomb energy may be computed directly from the Monte Carlo simulations. The second term concerns the rest of the whole 2D plane, the ‘‘unsampled primitive cells’’, for which we can *not* obtain the Coulomb energy directly from the simulation. In order to deal with the second region, we use the following trick.

The contribution from the second region may be written

$$\frac{E_{\text{unsmp}}}{N} = \frac{e^2}{2} \int_C d\mathbf{r} \int_U d\mathbf{r}' \frac{\langle \sum_{i \neq j} \delta(\mathbf{r} - \mathbf{r}_i) \delta(\mathbf{r}' - \mathbf{r}_j) \rangle}{|\mathbf{r} - \mathbf{r}'|}, \quad (\text{A2})$$

where \int_C means integral over the central primitive cell as in Eq. (3.3). Now, we assume that the correlation is negligible if the separation between \mathbf{r} and \mathbf{r}' is greater than some ‘‘correlation length’’ ξ_c . If the distance between the unsampled primitive cells (U) and the central primitive cell (C) is greater than ξ_c , we may use a Hartree approximation and write

$$\frac{E_{\text{unsmp}}}{N} = \frac{e^2}{2} \int_C d\mathbf{r} \int_U d\mathbf{r}' \frac{\rho(\mathbf{r})\rho(\mathbf{r}')}{|\mathbf{r} - \mathbf{r}'|}, \quad (\text{A3})$$

where we have defined the expectation value of the local density

$$\rho(\mathbf{r}) \equiv \sum_i \langle \delta(\mathbf{r} - \mathbf{r}_i) \rangle. \quad (\text{A4})$$

Note that the condition $i \neq j$ in Eq. (A2) is not needed, because the domains of \mathbf{r} and \mathbf{r}' are exclusive so that $\delta(\mathbf{r} - \mathbf{r}_i) \delta(\mathbf{r}' - \mathbf{r}_j) \delta_{ij} = 0$. Once the local density profile $\rho(\mathbf{r})$ is obtained in the central primitive cell from the

Monte Carlo simulations, the triangular periodicity leads to the density profile in the whole 2D plane, and Eq. (A3) can be explicitly computed.

Although the integral in Eq. (A3) diverges, this divergence is unphysical and is easily resolved by recalling that there is neutralizing background charge in real samples. Assuming uniform distribution for the positive background charge, the final form of the unsampled part is given by

$$\frac{E_{\text{unsmp}}}{N} = \frac{e^2}{2} \int_C d\mathbf{r} \int_U d\mathbf{r}' \frac{[\rho(\mathbf{r}) - \bar{\rho}][\rho(\mathbf{r}') - \bar{\rho}]}{|\mathbf{r} - \mathbf{r}'|}, \quad (\text{A5})$$

where $\bar{\rho}$ is the average density of electrons. The above integral is now well defined and can be computed using the Ewald sum method as in Refs. 33 and 35.

-
- ¹ E. P. Wigner, Phys. Rev. **46**, 1002 (1934).
² C. C. Grimes and G. Adams, Phys. Rev. Lett. **42**, 795 (1979).
³ D. Yoshioka and H. Fukuyama, J. Phys. Soc. Jpn. **47**, 394 (1979).
⁴ D. Yoshioka and P. A. Lee, Phys. Rev. B **28**, 4506 (1983).
⁵ H. A. Fertig, in *Perspectives in Quantum Hall Effects*, edited by S. das Sarma and A. Pinczuk (Wiley, New York, 1997).
⁶ D. C. Tsui, H. L. Störmer, and A. C. Gossard, Phys. Rev. Lett. **48**, 1559 (1982).
⁷ R. E. Prange and S. M. Girvin, *The quantum Hall effect*, 2nd ed. (Springer-Verlag, New York, 1990).
⁸ R. B. Laughlin, Phys. Rev. Lett. **50**, 1395 (1983).
⁹ H. W. Jiang *et al.*, Phys. Rev. Lett. **65**, 633 (1990).
¹⁰ V. J. Goldman, M. Santos, M. Shayegan, and J. E. Cunningham, Phys. Rev. Lett. **65**, 2189 (1990).
¹¹ M. B. Santos *et al.*, Phys. Rev. Lett. **68**, 1188 (1992).
¹² R. Price, P. M. Platzman, and S. He, Phys. Rev. Lett. **70**, 339 (1994).
¹³ X. Zhu and S. G. Louie, Phys. Rev. Lett. **70**, 335 (1993).
¹⁴ P. K. Lam and S. M. Girvin, Phys. Rev. B **30**, 473 (1984).
¹⁵ D. S. Fisher, B. I. Halperin, and R. Morf, Phys. Rev. B **20**, 4692 (1979).
¹⁶ E. Cockayne and V. Elser, Phys. Rev. B **43**, 623 (1991).
¹⁷ R. Price and P. M. Platzman, Phys. Rev. B **44**, 2356 (1991).
¹⁸ V. J. Goldman, M. Shayegan, and D. C. Tsui, Phys. Rev. Lett. **61**, 881 (1988).
¹⁹ H. Buhmann *et al.*, Phys. Rev. Lett. **66**, 926 (1991).
²⁰ R. G. Clark, Physica Scripta **T39**, 45 (1991).
²¹ I. V. Kukushkin *et al.*, Phys. Rev. B **45**, 4532 (1992).
²² E. M. Goldys *et al.*, Phys. Rev. B **46**, 7957 (1992).
²³ V. J. Goldman, J. K. Wang, B. Su, and M. Shayegan, Phys. Rev. Lett. **70**, 647 (1993).
²⁴ T. Sajoto *et al.*, Phys. Rev. Lett. **70**, 2321 (1993).
²⁵ L. Zheng and H. A. Fertig, Phys. Rev. B **50**, 4984 (1994).
²⁶ S. Kivelson, D.-H. Lee, and S.-C. Zhang, Phys. Rev. B **46**, 2223 (1992).
²⁷ S.-C. Zhang, S. Kivelson, and D.-H. Lee, Phys. Rev. Lett. **69**, 1252 (1992).
²⁸ L. Zheng and H. A. Fertig, Phys. Rev. Lett. **73**, 878 (1994).
²⁹ H. Yi and H. A. Fertig, unpublished.
³⁰ J. K. Jain, Phys. Rev. Lett. **63**, 199 (1989); “Composite Fermions,” in *Perspectives on Quantum Hall Effects*, S. Das Sarma and A. Pinczuk, eds., (John Wiley and Sons, New York, 1997).
³¹ S. M. Girvin and A. H. MacDonald, Phys. Rev. Lett. **58**, 1252 (1987); M.P.A. Fisher and D.H. Lee, Phys. Rev. B **39**, 2756 (1989).
³² K. Maki and X. Zotos, Phys. Rev. B **28**, 4349 (1983).
³³ L. Bonsall and A. A. Maradudin, Phys. Rev. B **15**, 1959 (1977).
³⁴ Our initial calculations of interstitial states using quantum Monte Carlo calculations reveal that, as in Ref. 28, Laughlin-Jastrow correlations between the interstitial electron and the lattice electrons significantly reduce their energy compared to Hartree-Fock estimates of the interstitial energy. However, it is found that the energy lowering is not great enough to account for what is seen in experiment when correlations exist only between the interstitial and lattice electrons, and not among the lattice electrons themselves. The instability with respect to interstitial formation just below $\nu = 1/m$ reported in Ref. 28 does not appear to occur in the more exact Monte Carlo evaluations of the energy. Nevertheless, the most significant conclusions of that work – the lowering of interstitial energies by Laughlin-Jastrow correlations and the resulting Hall insulating behavior – are unaffected by this problem.
³⁵ P. P. Ewald, Ann. Phys. (Leipz.) **54**, 519 (1917); **54**, 557 (1917); **64**, 253 (1921).
³⁶ R. Morf and B. I. Halperin, Phys. Rev. B **33**, 2221 (1986).
³⁷ N. Metropolis *et al.*, J. Chem. Phys. **21**, 1087 (1953).
³⁸ D. Levesque, J. J. Weis, and A. H. McDonald, Phys. Rev. B **30**, 1056 (1984).
³⁹ P. Chouquard and J. Clerouin, Phys. Rev. Lett. **50**, 2086 (1983).
⁴⁰ S. Kivelson, C. Kallin, D. P. Arovas, and J. R. Schrieffer, Phys. Rev. Lett. **56**, 873 (1986); Phys. Rev. B **36**, 1620 (1987); G. Baskaran, Phys. Rev. Lett. **56**, 2716 (1986); D. H. Lee, G. Baskaran, and S. Kivelson, Phys. Rev. Lett. **59**, 2467 (1987).
⁴¹ D. Ceperley, G. V. Chester, and M. H. Kalos, Phys. Rev. B **16**, 3081 (1977).
⁴² A similar approach to exchange in solid helium was developed in D. Ceperley, G. V. Chester, and M. H. Kalos, Phys. Rev. B **17**, 1070 (1978). An important distinction between our method and the one developed in this reference is that, because the magnetic field is absent in their problem, the single particle states could be taken to be real, so that there was no need to sample a phase.

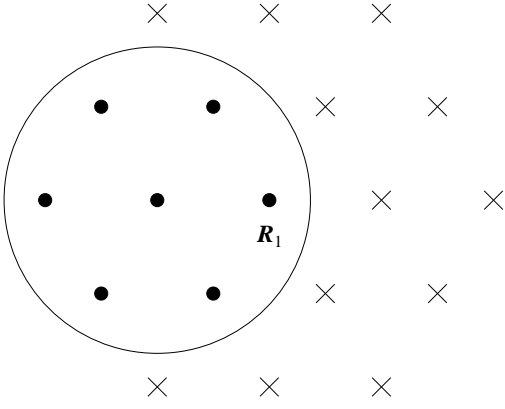


FIG. 1. An example of the underlying triangular lattice for a finite size WC. The large circle denotes the boundary of the physical disk and the filled dots the lattice sites, \mathbf{R}_i , within the disk. The crosses denote the positions of the ghosts, $\eta_j^{(1)}$, which balance the effective force at \mathbf{R}_1 .

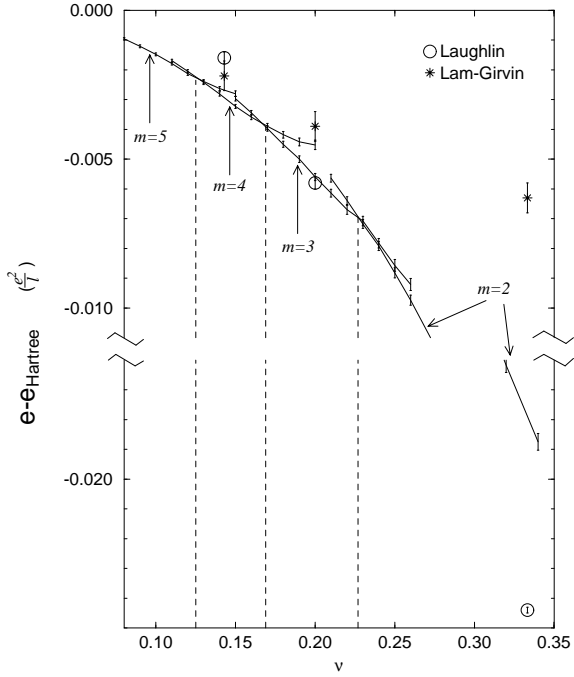


FIG. 2. The Coulomb energy per electron of the Laughlin-Jastrow-correlated Wigner crystal as a function of ν for various values of m . The energy is shown relative to that of the uncorrelated Hartree wavefunction ($m = 0$). The same quantity is presented for the Laughlin state (Ref. 14) and the Lam-Girvin wavefunction (Ref. 38) at $\nu = 1/3, 1/5$, and $1/7$. The dashed vertical lines represent the values of ν where the transition between different m states occur.

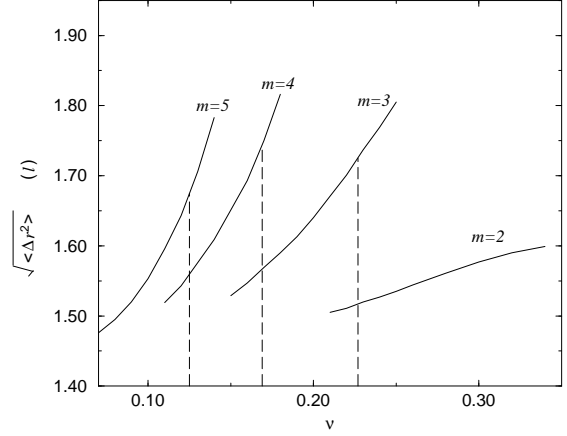


FIG. 3. Root-mean-square of the electron fluctuation from the lattice sites as a function of the filling factor ν . The dashed vertical lines represent the values of ν where the transition between different m states occur.

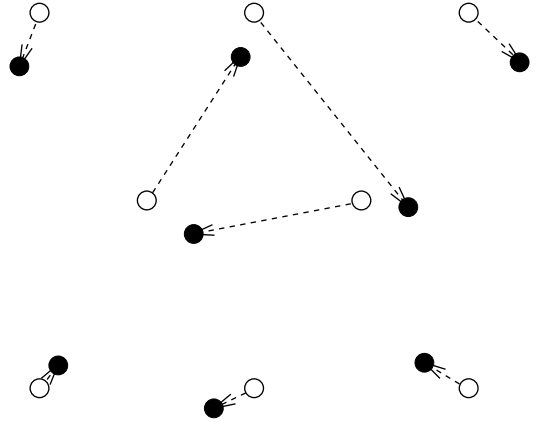


FIG. 4. A typical configuration of the three particle exchange ring which can be obtained from a “snap shot” of a Monte Carlo simulation. Electron positions are denoted by filled circles and lattice sites by empty circles. The arrows indicate which electron is originated from which Gaussian center \mathbf{R}_1 .

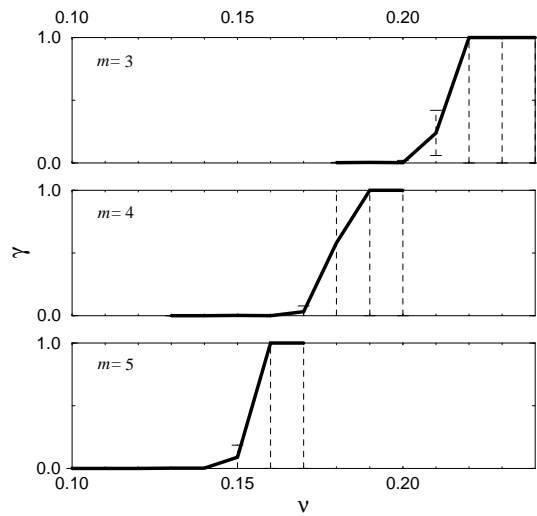


FIG. 5. Relative contribution of the exchange terms in the partition function. γ defined in (4.5) is plotted for several values of m . The dashed lines denote errorbars.